Dynamical origins for non-Gaussian vorticity distributions in turbulent flows

Michael Wilczek* and Rudolf Friedrich
Institute for Theoretical Physics, University of Münster, Wilhelm-Klemm-Strasse 9, 48149 Münster, Germany
(Received 11 December 2008; revised manuscript received 19 May 2009; published 27 July 2009; corrected 30 July 2009)

We present results on the connection between the vorticity equation and the shape and evolution of the single-point vorticity probability density function. The statistical framework for these observations is based on the classical hierarchy of evolution equations for the probability density functions by Lundgren, Novikov, and Monin combined with conditional averaging of the unclosed terms. The numerical evaluation of these conditional averages provides insights into the intimate relation of dynamical effects such as vortex stretching and vorticity diffusion and non-Gaussian vorticity statistics.

DOI: 10.1103/PhysRevE.80.016316 PACS number(s): 47.27.De, 47.10.−g, 47.27.E−

I. INTRODUCTION

One of the main goals of theoretical turbulence research is to develop a statistical nonequilibrium theory of turbulence from first principles. While this goal has not been achieved so far, many phenomenological theories exist, explaining a variety of phenomena of turbulent flows. For example, the classical K41 [1] theory manages to predict the observed energy spectrum, fails however to correctly predict more sophisticated statistical quantities. When striving for a statistical description of turbulence one is confronted with the fact that many turbulent observables display non-Gaussian statistics. For example, the probability density functions (PDFs) of the vorticity, the velocity gradient tensor or the Lagrangian acceleration exhibit heavy tails compared to a Gaussian PDF, showing that extreme events are orders of magnitudes more probable than in a Gaussian random field. In case of the vorticity this has been emphasized by Novikov more than four decades ago [2], demonstrating that the investigation of probability density functions is of particular use to characterize the statistics of turbulent flows [2–4]. Considering more than one spatial or temporal point as in case of Lagrangian or Eulerian velocity increments, the situation gets even more complicated. The PDFs then do not evolve self-similar in scale, but exhibit a scale-dependent shape. This fact, which is often referred to as intermittency, is accounted for in various phenomenological theories such as for example K62, the multifractal model [5], and a more recent approach focusing on Markovian properties of the velocity increment statistics [6]. Recently, there has been much effort in explaining possible mechanisms that lead to these non-Gaussian statistics. Based on works by Cantwell [7], Chevillard and Meneveau proposed a model for the stochastic evolution of the velocity gradient tensor, which compares well to numerical results [8]. Furthermore, Li and Meneveau suggested a simple dynamical model inspired by the Navier-Stokes equation, which shows remarkable similarities to statistics from real turbulence data [9,10]. While these phenomenological approaches give valuable insights and a rich characterization of the statistical properties of turbulence, they are not directly derived from the equation of motion of a fluid, i.e., the Navier-Stokes (or equivalently the vorticity) equation.

The above-mentioned classical works, however, make efforts to derive a statistical theory of turbulence from first principles. For example, Lundgren [3] and Monin [4] independently derived an evolution equation for the turbulent velocity with the help of PDF methods. Focusing on the vorticity, similar results were obtained by Novikov [2,11], almost at the same time. Extensions to turbulent combustion and many other applications were proposed by Pope [12]. Mathematically all these approaches have to face the famous closure problem of turbulence, which is inherent to the highly nonlinear and nonlocal character of the equations of motion. In Lundgren's work this problem results in an infinite hierarchy of evolution equations, involving an ever increasing number of velocities at different spatial points. In some of the works by Novikov a formal closure is achieved by introducing conditional averages, which enter the statistical equations as unknown functions.

It is mainly due to experimental efforts and direct numerical simulations of turbulence that today we know that turbulent flows are governed by coherent structures. In fully developed homogeneous isotropic three-dimensional turbulence, these structures appear as filamentary vortex tubes. Each of these tubes generates a swirling velocity field. The ensemble of vortices present in a turbulent fluid then interacts in a nonlinear manner, leading to the complex spatiotemporal structure of turbulent flows. In the interaction of these structures, some basic dynamical mechanisms can be identified: advection, vortex stretching, and viscous diffusion of vorticity.

It is a scope of the present work to establish a link between these dynamical aspects of turbulence and the non-Gaussian vorticity probability density functions. While the non-Gaussianity of the vorticity PDF is an established fact for a long time, we here put emphasis on revealing the quantities which determine the shape and evolution of the PDF. To this end, we present an evolution equation for the turbulent vorticity PDF in the spirit of Lundgren, Monin, and Novikov. The appearing conditional averages are evaluated with the help of highly resolved direct numerical simulations of the vorticity equation. The results help to highlight the connections between turbulent dynamics, coherent structures, and non-Gaussian statistics.

*mwilczek@uni-muenster.de

II. KINETIC THEORY FOR THE TURBULENT VORTICITY

The temporal evolution of the vorticity $\boldsymbol{\omega}(\boldsymbol{x},t)$ is governed by the vorticity equation,

$$\frac{\partial \boldsymbol{\omega}}{\partial t} + \boldsymbol{u}\cdot\boldsymbol{\nabla}\boldsymbol{\omega} = \boldsymbol{S}\cdot\boldsymbol{\omega} + \nu\Delta\boldsymbol{\omega} + \boldsymbol{F}, \tag{1}$$

where $\boldsymbol{u}(\boldsymbol{x},t)$ denotes the velocity field and $S_{ij}=\frac{1}{2}[\frac{\partial u_i}{\partial x_j}(\boldsymbol{x},t)+\frac{\partial u_j}{\partial x_i}(\boldsymbol{x},t)]$ denotes the rate-of-strain tensor. As we want to focus on incompressible fluids, the velocity field can be obtained from the vorticity field via Biot-Savart's law. ν denotes the kinematic viscosity and $\boldsymbol{F}(\boldsymbol{x},t)$ is an external forcing necessary to achieve a statistically stationary state. Starting from the fine-grained PDF $\hat{f}(\boldsymbol{\Omega};\boldsymbol{x},t)=\delta[\boldsymbol{\omega}(\boldsymbol{x},t)-\boldsymbol{\Omega}]$ [$\boldsymbol{\omega}(\boldsymbol{x},t)$ represents a realization of the vorticity field, whereas $\boldsymbol{\Omega}$ denotes the sample-space variable] standard PDF methods yield a kinetic equation for the turbulent vorticity PDF $f(\boldsymbol{\Omega};\boldsymbol{x},t)=\langle\hat{f}(\boldsymbol{\Omega};\boldsymbol{x},t)\rangle$ [2–4,11,12], which we will elucidate in the following. Similar derivations can be found in the literature [2–4]; it is however worthwhile following the basic steps in detail. Taking the temporal derivative of the fine-grained PDF one obtains

$$\frac{\partial}{\partial t}\delta(\boldsymbol{\omega}(\boldsymbol{x},t)-\boldsymbol{\Omega}) = -\boldsymbol{\nabla}_{\boldsymbol{\Omega}}\cdot\left\{\frac{\partial\boldsymbol{\omega}}{\partial t}\delta(\boldsymbol{\omega}(\boldsymbol{x},t)-\boldsymbol{\Omega})\right\}. \tag{2}$$

The advective term may be treated similarly, and hence we have

$$\frac{\partial}{\partial t}\hat{f} + \boldsymbol{\nabla}\cdot\{\boldsymbol{u}\hat{f}\} = -\boldsymbol{\nabla}_{\boldsymbol{\Omega}}\cdot\left\{\left(\frac{\partial\boldsymbol{\omega}}{\partial t}+\boldsymbol{u}\cdot\boldsymbol{\nabla}\boldsymbol{\omega}\right)\hat{f}\right\}, \tag{3}$$

$$= -\boldsymbol{\nabla}_{\boldsymbol{\Omega}}\cdot\{(\boldsymbol{S}\cdot\boldsymbol{\omega}+\nu\Delta\boldsymbol{\omega}+\boldsymbol{F})\hat{f}\}. \tag{4}$$

Here, incompressibility and Eq. (1) have been used. One now has the option to express the unclosed terms of this equation in terms of a coupling to the two-point PDF, as demonstrated in [2,3]. Determining an evolution equation for the two-point PDF then results in a coupling to the three-point PDF and so on. A second possibility is to express the unclosed terms in Eq. (3) in terms of conditional averages. Averaging Eq. (3) and using, e.g., $\langle\boldsymbol{u}\hat{f}\rangle=\langle\boldsymbol{u}|\boldsymbol{\Omega}\rangle f$ yields

$$\frac{\partial}{\partial t}f + \boldsymbol{\nabla}\cdot\{\langle\boldsymbol{u}|\boldsymbol{\Omega}\rangle f\} = -\boldsymbol{\nabla}_{\boldsymbol{\Omega}}\cdot\{\langle\boldsymbol{S}\cdot\boldsymbol{\omega}+\nu\Delta\boldsymbol{\omega}+\boldsymbol{F}|\boldsymbol{\Omega}\rangle f\}. \tag{5}$$

The right-hand side of this kinetic equation for the vorticity PDF reveals the different dynamical influences: the average vortex stretching term, vorticity diffusion, and the forcing conditioned on the sample-space vorticity. Taking into account homogeneity, the advective term vanishes, as both the conditional average as well as the PDF do not depend on the spatial coordinate. It is argued in [11] that the conditional average of the forcing times the vorticity decays rapidly with increasing Reynolds number. Given a sufficiently high Reynolds number, the large-scale forcing should not affect the smallest scales of the flow. As the coherent structures live on these scales, a negligible influence of the forcing is physically sound; numerical support for this approximation has also been given in [13]. Hence we will neglect the influence of the forcing in our following considerations. With these simplifications the kinetic equation reads

$$\frac{\partial}{\partial t}f = -\boldsymbol{\nabla}_{\boldsymbol{\Omega}}\cdot\{\langle\boldsymbol{S}\cdot\boldsymbol{\omega}+\nu\Delta\boldsymbol{\omega}|\boldsymbol{\Omega}\rangle f\}. \tag{6}$$

In order to achieve a statistically stationary state, the right-hand side of this equation has to vanish. This is only possible by a *statistical* cancellation of the appearing terms. In the following we will, in addition to homogeneity, consider isotropic turbulence. This imposes further constraints on the statistical quantities. It follows that $\langle\nu\Delta\boldsymbol{\omega}|\boldsymbol{\Omega}\rangle\sim\boldsymbol{\Omega}$. With $\langle\boldsymbol{S}\cdot\boldsymbol{\omega}|\boldsymbol{\Omega}\rangle=\langle\boldsymbol{S}|\boldsymbol{\Omega}\rangle\cdot\boldsymbol{\Omega}$, the conditioned rate-of-strain tensor can accordingly be written down as

$$\langle S_{ij}|\boldsymbol{\Omega}\rangle = g(\Omega)\delta_{ij} - 3h(\Omega)\frac{\Omega_i\Omega_j}{\Omega^2}, \tag{7}$$

with two scalar functions h and g only depending on the absolute value of the sample-space vorticity. The trace of this conditionally averaged tensor has to vanish, which yields $g=h$. It is easy to show that $\boldsymbol{\Omega}$ is an eigenvector of $\langle S_{ij}|\boldsymbol{\Omega}\rangle$, $\langle S_{ij}|\boldsymbol{\Omega}\rangle\Omega_j=-2g(\Omega)\Omega_i$ with the eigenvalue $\lambda_1=-2g(\Omega)$. The remaining eigenvalues can directly be determined due to the trace condition and isotropy, $\lambda_{2,3}=g(\Omega)$. It can be shown in a straightforward calculation that $g(\Omega)$ is related to the (normalized) rate of enstrophy production,

$$g(\Omega) = -\frac{1}{2}\left\langle\frac{\omega_i S_{ij}\omega_j}{\omega^2}\middle|\boldsymbol{\Omega}\right\rangle. \tag{8}$$

Now as $\langle\boldsymbol{S}|\boldsymbol{\Omega}\rangle\cdot\boldsymbol{\Omega}$ and $\langle\nu\Delta\omega|\boldsymbol{\Omega}\rangle$ both point into $\boldsymbol{\Omega}$ direction, a cancellation of the two terms on the right-hand side of Eq. (6) is possible in a statistical sense. While these observations show which dynamical effects statistically have to cancel, these equations do not suffice to directly calculate the vorticity PDF. This can be achieved by taking into account homogeneity of the flow. Calculating the Laplacian of the vorticity PDF yields

$$\frac{\partial^2}{\partial x_i^2}f = 0 = -\frac{\partial}{\partial\Omega_j}\left\langle\frac{\partial^2\omega_j}{\partial x_i^2}\middle|\boldsymbol{\Omega}\right\rangle f + \frac{\partial^2}{\partial\Omega_j\partial\Omega_k}\left\langle\frac{\partial\omega_j}{\partial x_i}\frac{\partial\omega_k}{\partial x_i}\middle|\boldsymbol{\Omega}\right\rangle f. \tag{9}$$

An appealing equation arises, when combining the kinetic Eq. (6) with homogeneity relation (9). For homogeneous turbulent flows, the temporal evolution of the vorticity PDF can then be described by

$$\frac{\partial}{\partial t}f = -\frac{\partial}{\partial\Omega_i}\langle S_{ij}\omega_j|\boldsymbol{\Omega}\rangle f - \frac{\partial^2}{\partial\Omega_i\partial\Omega_j}\left\langle\nu\left(\frac{\partial\omega_i}{\partial x_k}\frac{\partial\omega_j}{\partial x_k}\right)\middle|\boldsymbol{\Omega}\right\rangle f, \tag{10}$$

where the terms on the right-hand side are related to the production and dissipation of vorticity (or enstrophy). Further information on the PDF is obtained by studying the nonstationary case of Eq. (6) with the method of characteristics. The ordinary differential equation for the characteristics reads

TABLE I. Major simulation parameters. Number of collocation points N, Reynolds number based on the Taylor microscale R_λ, root-mean-square velocity u_{rms}, kinematic viscosity ν, integral length scale L, large-eddy turnover time T, Kolmogorov length scale η, and Kolmogorov time scale τ_η. $k_{\max}\eta$ characterizes the spatial resolution of the smallest scales.

N	R_λ	u_{rms}	ν	L	T	η	τ_η	$k_{\max}\eta$
512	164	0.082	0.0001	2.19	26.7	0.0079	0.63	1.6

$$\dot{\mathbf{\Omega}} = \langle \boldsymbol{S}\cdot\boldsymbol{\omega} + \nu\Delta\boldsymbol{\omega}|\mathbf{\Omega}\rangle, \tag{11}$$

with the solution describing the temporal evolution of the sample-space vorticity.

For the comparison with our numerical simulation we consider the theory for the PDF of a single component of the vorticity, say, $f(\Omega_x;t)$. Equation (6) then reduces to

$$\frac{\partial}{\partial t}f = -\frac{\partial}{\partial \Omega_x}\{\langle(\boldsymbol{S}\cdot\boldsymbol{\omega} + \nu\Delta\boldsymbol{\omega})_x|\Omega_x\rangle f\}. \tag{12}$$

The statistical evolution of the sample-space vorticity Ω_x is accordingly given by

$$\dot{\Omega}_x = \langle(\boldsymbol{S}\cdot\boldsymbol{\omega})_x + \nu\Delta\omega_x|\Omega_x\rangle, \tag{13}$$

i.e., by the sum of the conditionally averaged vortex stretching term and the conditionally averaged vorticity diffusion. In case of a single component, homogeneity implies

$$0 = -\frac{\partial}{\partial \Omega_x}\langle\Delta\omega_x|\Omega_x\rangle f + \frac{\partial^2}{\partial \Omega_x^2}\langle(\nabla\omega_x)^2|\Omega_x\rangle f, \tag{14}$$

which suffices to determine the functional form of the vorticity PDF for homogeneous (and not necessarily stationary) flows [14]. Inserting this into Eq. (12) gives

$$\frac{\partial}{\partial t}f = -\frac{\partial}{\partial \Omega_x}\langle(\boldsymbol{S}\cdot\boldsymbol{\omega})_x|\Omega_x\rangle f - \frac{\partial^2}{\partial \Omega_x^2}\langle\nu(\nabla\omega_x)^2|\Omega_x\rangle f, \tag{15}$$

which yields the stationary solution

$$f(\Omega_x) = \frac{\mathcal{N}}{\langle\nu(\nabla\omega_x)^2|\Omega_x\rangle}\exp\left(-\int_{-\infty}^{\Omega_x} d\Omega_x' \frac{\langle(\boldsymbol{S}\cdot\boldsymbol{\omega})_x|\Omega_x'\rangle}{\langle\nu(\nabla\omega_x)^2|\Omega_x'\rangle}\right), \tag{16}$$

with a normalization constant $\mathcal{N}$. This shows that in a stationary homogeneous flow the vorticity PDF is determined by the dynamical effect of vortex stretching and the vorticity gradient (which is related to the dissipation of vorticity). In the following, we numerically evaluate the conditionally averaged vortex stretching term $\langle(\boldsymbol{S}\cdot\boldsymbol{\omega})_x|\Omega_x\rangle$, vorticity diffusion $\langle\nu\Delta\omega_x|\Omega_x\rangle$, and squared vorticity gradient $\langle\nu(\nabla\omega_x)^2|\Omega_x\rangle$.

III. NUMERICAL EVALUATION

The turbulent fields under consideration in the present work are generated by a standard dealiased Fourier-pseudo-spectral code [15,16] for the vorticity equation. The integration domain is a triply periodic box of box length 2π. To obtain a statistically stationary flow we apply a large-scale forcing. The time-stepping scheme is a third-order Runge-Kutta scheme [17].

For the present work, we conduct two different types of simulations. For an estimation of the conditional averages determining the stationary PDF a run in the statistically stationary regime is performed; Table I sums up the major simulation parameters. In order to gain deeper insights into the formation of the PDF a second nonstationary run with comparable simulation parameters is performed. The initial condition of this run exhibits a Gaussian vorticity distribution and the same energy spectrum as the statistically stationary simulation. The field evolves under the dynamics of the vorticity equation and during the relaxation to the statistically stationary state the non-Gaussian vorticity PDF emerges.

Regarding the stationary situation, Fig. 1 shows the numerically evaluated conditional averages of Eqs. (15) and (12). The conditionally averaged vortex stretching term is positively correlated with the vorticity component, while the conditionally averaged vorticity diffusion shows strong anticorrelations. These tendencies can be physically understood; in presence of strong vorticity the vortex stretching term causes a (self-)amplification of vorticity, the diffusive term then tends to deplete this vorticity.

Checking the validity of Eq. (16) with our numerical data, the comparison of the directly estimated and reconstructed vorticity PDF is depicted in Fig. 2. A good agreement over seven orders of magnitude is given. As Eq. (15) yields a Gaussian in case of $\langle(\boldsymbol{S}\cdot\boldsymbol{\omega})_x|\Omega_x\rangle \sim \Omega_x$ and $\langle\nu(\nabla\omega_x)^2|\Omega_x\rangle$

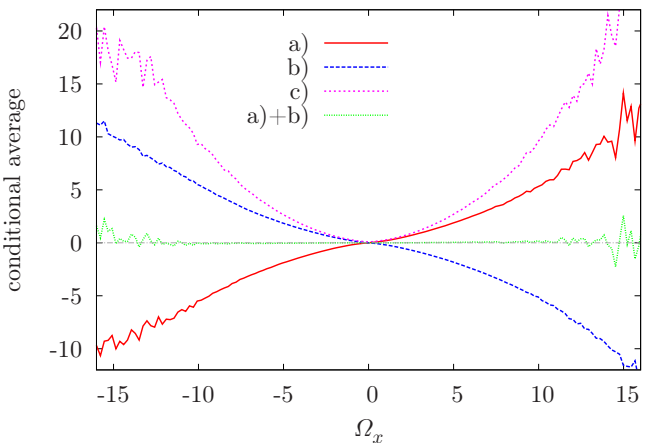

FIG. 1. (Color online) (a) Conditional averages of the vortex stretching term $\langle(\boldsymbol{S}\cdot\boldsymbol{\omega})_x|\Omega_x\rangle$, (b) the vorticity diffusion $\langle\nu\Delta\omega_x|\Omega_x\rangle$, and the sum of both terms. The sum (approximately) vanishes, as required for statistical stationarity. The squared vorticity gradient (c) $\langle\nu(\nabla\omega_x)^2|\Omega_x\rangle$ exhibits a strong dependence on Ω_x.

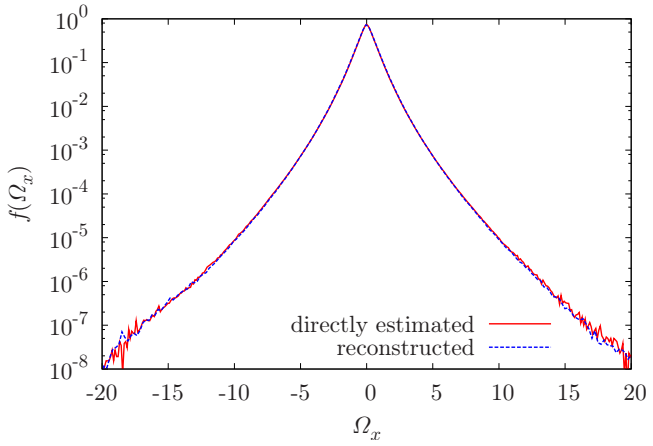

FIG. 2. (Color online) Logarithmic plot of the vorticity PDF estimated directly from our data and the reconstructed PDF according to Eq. (15). The agreement over several orders of magnitude is excellent; slight deviations are visible in the far tails of the PDF.

$\sim$const., the highly non-Gaussian shape of the vorticity PDF can be tracked down to the strong Ω_x dependence of $\langle(\nu\nabla\omega_x)^2|\Omega_x\rangle$. Further motivation for the functional form of the conditional averages can be given when examining the basic structures present in the flow. As the visualizations in Fig. 3 suggest, the flow consists of elongated vortex tubes, which can be modeled with Burgers vortices [18]. A Burgers vortex exhibits a vorticity field according to

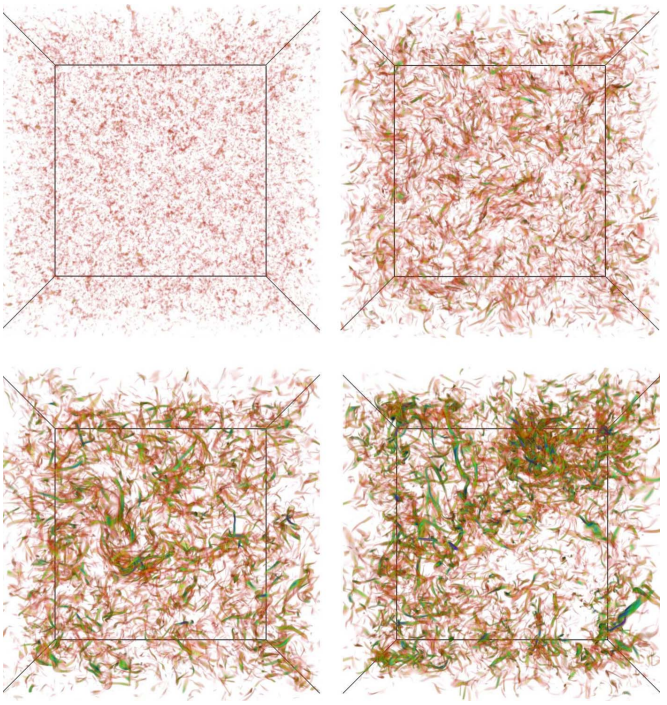

FIG. 3. (Color online) Volume rendering of the absolute value of vorticity above a fixed threshold for different stages of the nonstationary simulation (from top left to bottom right: initial condition, $0.11T$ (200 time steps), $0.38T$ (600 time steps), and $3.53T$ (6000 time steps). Volume rendering produced with VAPOR, www.vapor.ucar.edu.

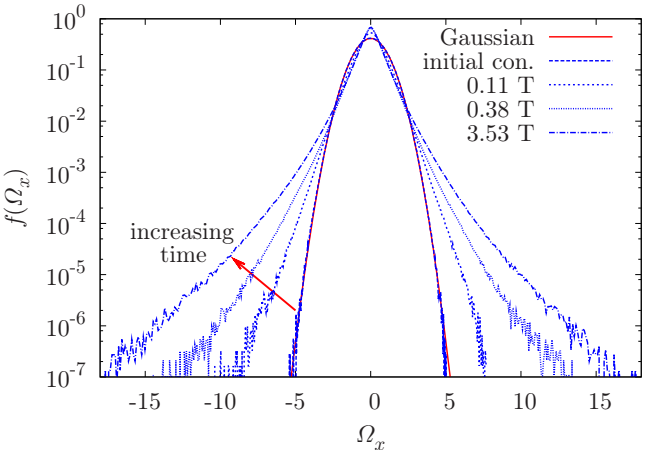

FIG. 4. (Color online) Temporal evolution of the vorticity PDFs from a Gaussian initial condition. Pronounced tails emerge during the course of the simulation.

$$\boldsymbol{\omega} = \omega(r)\boldsymbol{e}_z = \frac{\Gamma a}{4\pi\nu} e^{-ar^2/4\nu}\boldsymbol{e}_z, \tag{17}$$

characterized by the strain parameter a and circulation Γ. For this structure the vortex stretching term and the squared vorticity gradient are readily calculated to

$$\boldsymbol{S}\cdot\boldsymbol{\omega} = a\boldsymbol{\omega} \tag{18}$$

and

$$(\nabla\omega_z)^2 = \left(\frac{\partial}{\partial r}\boldsymbol{\omega}\right)^2 = \frac{a^2r^2}{4\nu^2}\boldsymbol{\omega}^2. \tag{19}$$

That means, for fixed a, Γ, and ν, the vortex stretching term is a linear function of the vorticity, whereas the squared vorticity gradient turns out to be a quadratic function of the vorticity. Thinking of turbulence as an ensemble of Burgers-like vortices, this picture already captures the main features of the conditional averages shown in Fig. 1. Deviations from this simple argument are possible due to the fact that the circulation of a vortex tube in a turbulent flow is not independent of the surrounding strain field and that straight vortex tubes are not the only structures present.

While helping to explain the non-Gaussian nature of the turbulent vorticity, the above considerations give no direct information on how the dynamical processes of vortex stretching and vorticity diffusion go along with the formation of the characteristic shape of the PDF. To elucidate this issue, we turn to the nonstationary simulation starting with a vorticity field exhibiting a Gaussian distribution. Under the temporal evolution of the vorticity Eq. (1) strong spatiotemporal correlations in form of, e.g., vortex tubes are generated and the initial Gaussian distribution relaxes to the non-Gaussian PDF observed for the statistically stationary regime, as illustrated in Fig. 4. The temporal evolution of the vorticity field is visualized in Fig. 3. The initial condition with the Gaussian PDF appears unstructured, but already at $0.11T$ the emergence of small vorticity worms can be observed. In the course of the simulation these structures grow stronger, after $0.38T$ thin vortex tubes can be observed. Interestingly these

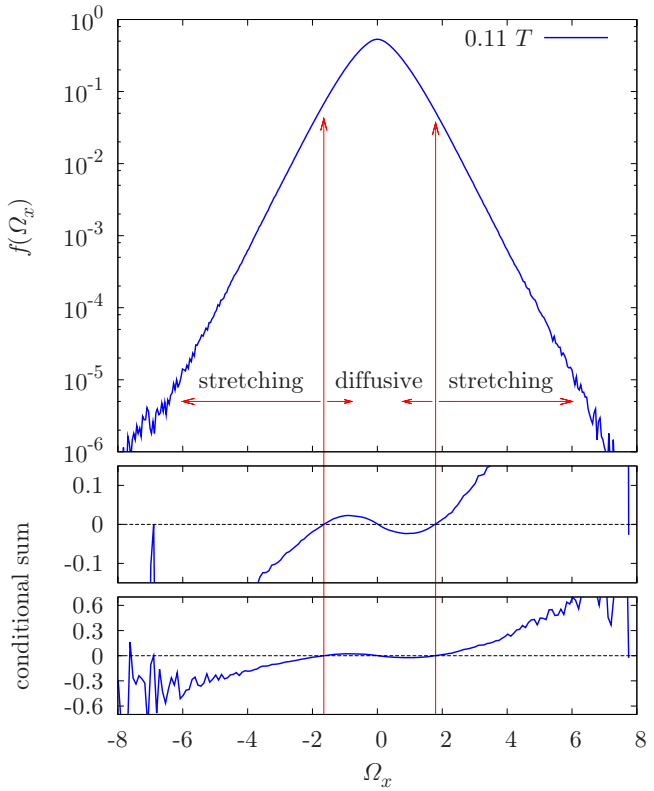

FIG. 5. (Color online) Illustration of the deformation of the PDF for the nonstationary simulation. Upper figure: The vorticity PDF for $0.11T$ is already non-Gaussian, yet has not developed strong tails. Lower figures: conditional sum $\langle(\boldsymbol{S}\cdot\boldsymbol{\omega})_x+\nu\Delta\omega_x|\Omega_x\rangle$ shown for two different y ranges. The inner region of the vorticity PDF is quenched together due to dominant vorticity diffusion while the outer regions are stretched toward higher vorticity values due to dominant vortex stretching.

tubes tend to cluster, as can be seen in the snapshot taken at $3.53T$.

The temporal evolution of the sum of the conditional averages of Eq. (12) is evaluated for the nonstationary situation. An example for $0.11T$ is depicted in the lower part of Fig. 5. As expected, the sum of both averages does not cancel like in the statistically stationary run. While the initial condition is diffusion dominated as the vortex stretching has not started generating structures, the formation of two distinct regions (separated by the zero crossings of the conditional sum) may be observed in the course of the simulation. Low absolute values of the vorticity are dominated by the conditional vorticity diffusion while larger absolute values are amplified due to a dominant vortex stretching. This subtle detail remains as the PDF is approaching stationarity; however the two terms tend to cancel more and more. After reaching the statistically stationary state the statistical balance of the conditional averages is recovered. How the unbalanced conditional sum affects the formation of the PDF may be interpreted with the method of characteristics from Fig. 5. The inner diffusively dominated region is quenched toward zero vorticity, while the outer vortex stretching dominated regions are stretched toward larger absolute values of vorticity. The emerging physical picture fits well to the common understanding of turbulent flows. The stretching of the PDF toward larger absolute values of vorticity corresponds to the amplification of vortex filaments due to vortex stretching. The lower-valued vorticity, which corresponds to more unstructured regions of the flow, is depleted by the diffusive term. Hence the formation of the non-Gaussian vorticity PDF hereby is related to the interplay of the two physical mechanisms of vortex stretching and vorticity diffusion.

IV. SUMMARY

To summarize, we reported on theoretical and numerical results on the link between the vorticity equation, coherent structures, and the non-Gaussian distribution of vorticity. Based on classical works by Lundgren, Novikov, and Monin an investigation of the kinetic equation of the one-point vorticity PDF reveals that the conditional averages of vortex stretching and vorticity diffusion determine the temporal evolution and shape of the vorticity PDF. A closed expression for the stationary vorticity PDF was found in terms of the conditional averages of vortex stretching and the squared vorticity gradient. Numerical simulations confirm this relation with a high degree of precision. Further investigations of a nonstationary flow reveal that during the transition to the stationary state, two distinct regions of the vorticity PDF can be found: the inner region of this PDF is quenched due to dominant vorticity diffusion while the development of the fat tails can be associated with the stretching of strong vortices.

Hence this work highlights a direct connection between basic dynamical features of turbulence and their statistical consequences. These results encourage studying turbulent flows in terms of coherent structures as a main source for non-Gaussian statistics.

ACKNOWLEDGMENTS

We acknowledge insightful discussions with F. Jenko, O. Kamps, M. Voßkuhle, and A. Daitche. Computational resources are allocated at the LRZ Munich (Project No. h0963) and on the BOB cluster at RZ Garching.

[1] A. N. Kolmogorov, Proc. R. Soc. London, Ser. A **434**, 9 (1991).
[2] E. A. Novikov, Sov. Phys. Dokl. **12**, 1006 (1968).
[3] T. S. Lundgren, Phys. Fluids **10**, 969 (1967).
[4] A. Monin, Prikl. Mat. Mekh. **31**, 1057 (1967).
[5] U. Frisch, *Turbulence—The Legacy of A.N. Kolmogorov* (Cambridge University Press, Cambridge, England, 1995).
[6] R. Friedrich and J. Peinke, Phys. Rev. Lett. **78**, 863 (1997).
[7] B. J. Cantwell, Phys. Fluids A **4**, 782 (1992).
[8] L. Biferale, L. Chevillard, C. Meneveau, and F. Toschi, Phys.

Rev. Lett. **98**, 214501 (2007).
[9] Y. Li and C. Meneveau, Phys. Rev. Lett. **95**, 164502 (2005).
[10] Y. Li and C. Meneveau, J. Fluid Mech. **558**, 133 (2006).
[11] E. A. Novikov, Fluid Dyn. Res. **12**, 107 (1993).
[12] S. Pope, *Turbulent Flows* (Cambridge University Press, Cambridge, England, 2000).
[13] E. A. Novikov and D. Dommermuth, Mod. Phys. Lett. B **8**, 1395 (1994).
[14] E. S. C. Ching, Phys. Rev. E **53**, 5899 (1996).
[15] C. Canuto, M. Hussaini, A. Quarteroni, and T. Zang, *Spectral Methods in Fluid Dynamics* (Springer-Verlag, Berlin, 1987).
[16] T. Y. Hou and R. Li, J. Comput. Phys. **226**, 379 (2007).
[17] C-W. Shu and S. Osher, J. Comput. Phys. **77**, 439 (1988).
[18] J. Burgers, *Advances in Applied Mechanics* (Academic, New York, 1948).